The distribution of O and N in the surface region of laser-patterned titanium revealed by atom probe tomography

Applied Surface Science 562 (2021) 150193

Contents lists available at ScienceDirect

Applied Surface Science

journal homepage: www.elsevier.com/locate/apsusc

Short Communication

The distribution of O and N in the surface region of laser-patterned titanium revealed by atom probe tomography

D. Kuczyńska-Zemła [a,*], G. Sundell [b], M. Zemła [a], M. Andersson [b], H. Garbacz [a]

[a] Faculty of Materials Science and Engineering, Warsaw University of Technology, Wołoska 141, 02-507 Warsaw, Poland
[b] Applied Chemistry, Dept. Chemistry and Chemical Engineering, Chalmers University of Technology, SE-41296 Gothenburg, Sweden

ARTICLE INFO

Keywords:
Titanium
Atom probe tomography
Oxidation
Laser treatment
Bone implant

ABSTRACT

Direct Laser Interference Lithography (DLIL) has shown to be a promising technique to chemically and physically alter the surface of titanium. In this work, atom probe tomography analysis was performed on DLIL-treated titanium to obtain the chemical composition of the surface in maxima and minima interference positions. The analysis revealed that a multilayer structure consisting of oxide/oxynitride is formed at both positions; however, the chemical composition is altered differently between the two. The observed difference is believed to be due to an uneven heating and temperature distribution, which is demonstrated by thermal simulations.

1. Introduction

Amongst a variety of laser techniques, Direct Laser Interference Lithography (DLIL) has attracted great deal of attention. This is due to its flexibility to modify various types of materials [1–5] and for creating diversified surface topographies [6]. DLIL treatment can improve mechanical [7], optical [8] or biological properties [9,10] of surfaces, and has therefore been of interest in various applications. The pulsed DLIL method enables surface texturing with limited surface heating [7] and can provide thousands of patterns in one step. For example, titanium is melted only at the maximum intensity positions (constructive interference) for a very short time and the molten material is then transferred through Marangoni convection out to the interference minima positions (destructive interference) creating characteristic periodic patterns [11,12]. The mechanism behind the surface texturing and pattern formation during DLIL processing strongly depends on the applied laser fluence, which are either Marangoni convection (for moderate laser fluences) or the recoil pressure (laser fluence exceeds the evaporation temperature of the material [2,11,12]). It has previously been reported that for the ns-pulses the structuring mechanism is based on Marangoni convection [13]. It means that due to the local surface heating at the interference maxima positions, severe temperature gradients occur on the surface. The temperature gradient causes a tension gradient to appear on the surface, which leads the flow of molten material at the maxima toward the colder areas at the minima positions. If the amount of molten material at the maxima position is enough to cover the whole distance to the minima position it results in a characteristic round-shaped periodic pattern.

The physicochemical properties of the surface are among the most important factors influencing bone anchoring of biomedical implants for joint replacement [14]. In recent years, great effort has therefore been put on the analysis of the chemical composition of the titanium surface and its influence on the biological response [14–16]. In the case of titanium implants, the surrounding biological medium (for example proteins and cells) will interact with the native titanium oxide, which is composed mainly of TiO_2 [17,18]. Lower oxide states are also present on the surface and the thickness of the oxide layer is typically less than 10 nm [17,19]. It has been demonstrated that during any laser treatment, the surface characteristics are influenced by varying the laser modification parameters [9,20,21]. In addition, during DLIL treatment, uneven heating and temperature distribution of the titanium surface, as caused by the interference phenomenon, may lead to inhomogeneity of the chemical composition and periodically modulated film thickness at the intensity maxima/minima positions.

Although many studies have been performed examining the chemical composition of DLIL-modified titanium surfaces [9,22], work assessing direct analysis of the oxides formed at the maxima/minima interference positions is much less frequent. Studies show that the nitrogen content in the titanium reactive layer can be altered by changing the working conditions of the laser [9,21]. Moreover, our previous studies, using X-ray photoelectron spectroscopy (XPS), have revealed presence of titanium oxides and nitrides/oxynitrides on DLIL-treated

* Corresponding author.
E-mail address: donata.kuczynska-zemla.dokt@pw.edu.pl (D. Kuczyńska-Zemła).

https://doi.org/10.1016/j.apsusc.2021.150193
Received 11 February 2021; Received in revised form 19 May 2021; Accepted 20 May 2021
Available online 26 May 2021

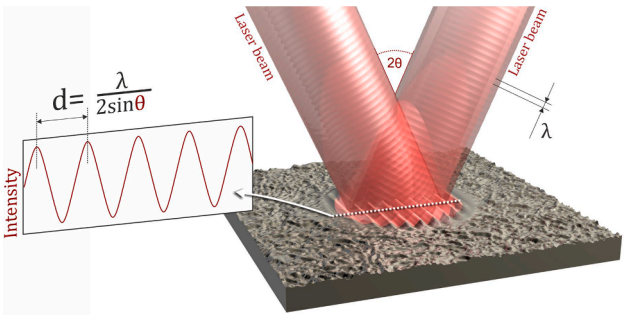

Fig. 1. Scheme of the Direct Laser Interference Lithography DLIL.

titanium surfaces [7,23]. However, XPS, which is known for its high surface sensitivity and low penetration depth, can only confirm the presence of titanium nitride/oxynitride phases and not their spatial distribution [9,24,23]. Also, spectroscopy in transmission electron microscopy (TEM) is also challenging in case of light-weight elements such as oxygen and nitrogen and does not have sufficient chemical sensitivity to accurately quantify their concentrations. Therefore, we have chosen to use atom probe tomography (APT), which has the capability of providing chemical composition analysis with high lateral resolution. The use of APT has during recent years been broadened to the areas of oxides analysis [25] and even bio-interfaces of titanium implants [26,27].

2. Materials and methods

2.1. Laser treatment

To examine the chemical composition of DLIL-modified titanium selectively at the interference maxima and minima positions, a pulsed Nd:YAG solid-state laser system with a wavelength of 1064 nm, a pulse duration of 8–10 ns, and a pulse repetition rate of 10 Hz was used. A dielectric beam-splitter was used to split the primary laser beam into two beams, which were utilized to create a grooved pattern on the titanium substrate. The laser surface functionalization was performed in air atmosphere with laser energy of approx. 400 mJ and 7 repetitions using shot peened and acid etched pre-treated samples. The laser fluence was set to approximately 350 mJ cm^{-2}. The two different pre-treatments (shot peening and acid etching) were applied to demonstrate that DLIL is possible to perform on commercial implants, where such treatments are commonly used to structure the surface [22,28]. The laser treatment process is schematically presented in Fig. 1. As a result of the performed DLIL, well-defined and symmetrical grooves with a depth of 1.0–1.5 μm and a period of 6–7 μm were formed, independently of the topography after shot peening and acid etching [7,23,29]. This indicates that DLIL can be used as the final surface modification step to create specific surface topographies on existing commercial implants in order

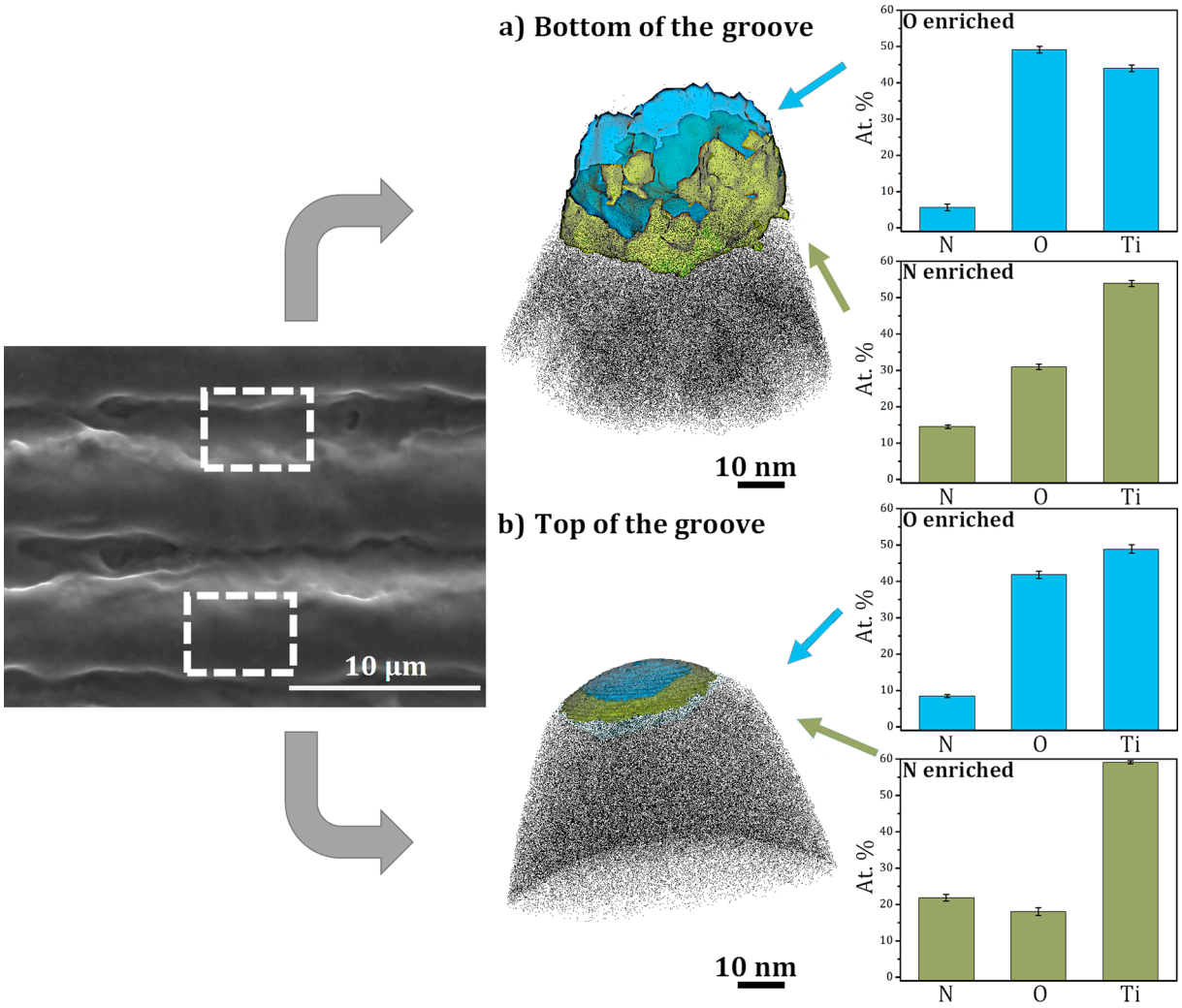

Fig. 2. SEM micrograph of the DLIL-modified titanium with detailed APT analysis providing the distributions of the elements, (a) intensity maximum of DLIL sample, (b) intensity minimum of DLIL sample, Ti-containing ions are displayed in black.

to induce the desired biological reaction. The dimension of the grooves was selected based on previous reports, which have shown increased osteoblasts alignment when they are in the range of 1–10 μm in width [30,31] with varying depths [32]. The arithmetic surface roughness, Ra, before and after DLIL were determined by optical profilometry and were found to be 0.9 and 0.6 μm, respectively.

2.2. Atom probe tomography

Since the analyzed volume in a typical APT measurement is very small (approximately 50 × 50 × 200 nm), a high precision is required for the sample preparation. Hence, specimens including both the intensity maximum and minimum positions of a laser-patterned surface were prepared using a focused ion beam (FIB) lift-out technique with subsequent ion beam tip sharpening in accordance with established procedures [33,34]. In order to protect the surface before FIB preparation, a 200 nm thick gold-capping layer was deposited on the titanium surface by magnetron sputtering. A 15 × 2 × 3 μm wedge was milled out, using a monoisotopic $^{69}Ga^{+}$ beam operated at 30 kV acceleration voltage, and retrieved with an Omniprobe needle from the bottom and the top of the DLIL-modified titanium surface grooves. Slices of the wedge were attached to prefabricated Si posts by means of Pt deposition. Needle-shaped specimen were then prepared by milling annular patterns with decreasing radii and beam currents, until the tip apex radii were approximately 50 nm. Finally, a cleaning step at 2 kV and 8 pA was performed. Atom probe analysis was performed using an Imago LEAP 3000X HR instrument operated in laser pulsed mode with green light (λ = 532 nm). The laser pulsing frequency was 100 kHz and the pulse energy was 0.3–0.5 nJ. The tips were held at a base temperature of approx. 50 K during analysis. Scanning electron microscope (SEM) micrographs were used to estimate the evolution of the tip radii for the reconstructions. The three-dimensional (3D) reconstructions were based on SEM images of the tip geometry. Reconstructions were made using the IVAS 3.6.6 software (Cameca, US). Five tips were prepared for each position, out of which three reconstructions contained the investigated region.

2.3. Thermal simulations

In order to investigate the thermal distribution on the surface during of the laser-treatment, simulations of the thermal profile were carried out.

Based on the 1st law of thermodynamics, expressed as continuity equation of the heat flux, combined with Fourier's law, one can derive the heat equation:

$$\rho c_p \frac{\partial T}{\partial t} = Q + \nabla(\kappa \nabla T) \quad (1)$$

where $T = T(x, z, t)$ is the temperature at a particular place in a space (x, z) and time (t); ρ, c_p, and κ stands for density, specific heat capacity, and thermal conductivity, respectively; Q is a term including the heat source and the heat required to go through the phase change (melt/vaporize or alotropic transformation) by the laser-treated material. The finite-difference methods were used for solving these differential equations. The following assumptions were made: (1) material's properties are constant (independent of temperature, phase and time); (2) there is no radiation from the surface; (3) convection in the melt and outside material is not accounted for; (4) the heat source has a Gaussian distribution (in time) and is generated by the absorbed material 5 peaks of the laser interference pattern. The model description is elaborated in the supplementary material.

3. Results and discussion

3.1. Atom probe tomography

Fig. 2 presents the surface morphology and the 3D reconstruction of an APT analysis obtained from the bottom (maximum intensity position) and top (minimum intensity position) of the groove. For both intensity positions two distinct layers were observed in the surface region with different stochiometric compositions. A clear N-rich layer was observed between the oxygen layer (O-rich) and Ti-metal in the APT 3D reconstructed volume. As we are not able to retain crystallographic information from the APT reconstructions of the N-rich layer, we cannot determine the exact phase structure. Isoconcentration surfaces at the bottom of the groove were set to 36 at.% of oxygen and 10 at.% of nitrogen content in O-rich and N-rich regions, respectively. At the top of the groove these two were 31 at.% of oxygen and 14 at.% of nitrogen. The selection of these parameters consisted of creating the largest possible continuous layers containing O and N atoms. The APT analysis shows that there is a significant difference in the stoichiometric chemical composition between the two regions, which probably is a result of the uneven temperature distribution at the irradiated surface. In the O-rich layer for both intensity positions, the measured Ti/O ratio is close to 1 and with the presence of nitrogen. In the N-rich layer at the bottom of the groove, N levels do not exceed O levels, suggesting some kind of oxynitride phase at this intensity position. At the top of the groove, the content of oxygen is lower compared to the nitrogen, which content did not exceed 25 at.%. This is interesting, since as stated by Wang *et al.* [35] the formation of a N-rich layer may highly influence the surface properties of the modified titanium substrate.

Laser surface texturing is a non-equilibrium process due to the extremely fast heating and cooling rates [36]. The laser induced temperature may significantly exceed the melting point of the substrate. Melting of the titanium results in an interaction of the liquid phase with the components of the air – oxygen and nitrogen. There are several studies describing light element insertion into titanium during laser processing [20,21,37–39]. Torrent *et al.* [20] showed that at 1064 nm wavelength there is higher efficiency for N insertion. Lavisse *et al.* [39] concluded that shorter pulses duration favours the insertion of nitrogen into the titanium substrate. Additionally, authors' claim [39] that the amount of light elements (oxygen and nitrogen) inserted into titanium increased with an increased laser fluence. A recent experimental study on laser treated titanium presented an oxygen enriched layer at the outermost surface, while nitrogen diffusion-enriched zone existed beneath the O-rich layer [38] which is quantitatively similar to our APT results. The formation enthalpies of TiN and TiO_2 are −338 and −944 kJ/mol, respectively, indicating greater thermodynamic stability of the oxides [40]. However, according to Zeng *et al.* [38] during laser processing of titanium, TiN appears prior to oxides [38]. This, since titanium nitride is more stable compared to titanium oxide at elevated temperatures (>2350°C) as provided by Ti-N and Ti-O phase diagrams [38]. Titanium oxide (TiO_2) is thus formed during the cooling process as a result of solidification of the pre-existing liquid titanium or the reaction between TiN and O_2 [38]. Oxygen atoms diffuse into the TiN lattice and replace nitrogen atoms and forms a thin TiO_2 layer near the surface. Otherwise, in order to insert N into the substrate there must be a plasma which dissociate nitrogen and the substrate must be melted. The insertion of nitrogen also requires the presence of reactive N in the plasma [21]. A higher diffusion coefficient of nitrogen in the titanium oxide and slower dissolution in the titanium substrate compared to the oxygen, causes that nitrogen to accumulate near the interface metal/oxide [21,37]. The smaller enthalpy of titanium oxides compared to nitrides indicates that oxygen diffusion into the metallic substrate is limited and therefore oxides are formed near to the uppermost surface [41].

During DLIL treatment, heating/melting of the titanium surface is very localized, and the temperature is highest at the interference maxima [3]. Both the oxidation and nitridation processes that are taking

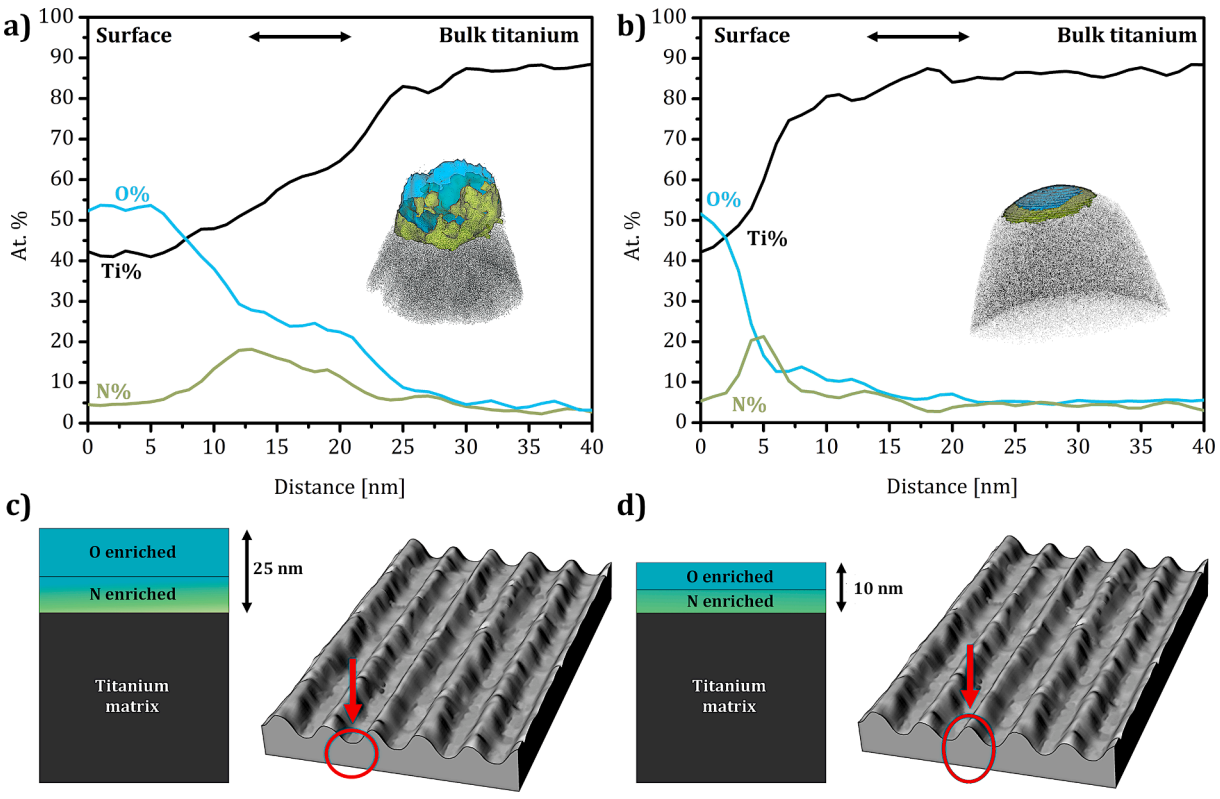

Fig. 3. 1D concentration profiles of Ti, O, and N ranging from the oxide layer into the bulk titanium as obtained from the APT 3D reconstruction, (a) maximum intensity position, (b) minimum intensity position, (c, d) schematic representation of the depth of chemical composition changes.

place during melting of the titanium are diffusion dominated. In comparison between the two interference positions it is evident that there is a higher oxygen content at the bottom of the groove, which probably is due to the higher operating temperature allowing higher diffusion times of O atoms into the layer. The differences in content of the individual elements in the N-rich layer strongly depends on the diffusion process and operating temperature. These findings provide additional necessity to analyze the chemical composition in these layers and how it is affected by the different laser intensities. Fig. 3 presents a comparison of one-dimension (1D) concentration profiles for the minima/maxima intensity positions on the DLIL-treated sample. Interestingly, there is a difference in the thickness of detected double layer system between two analyzed positions. For the maximum intensity position, changes in the chemical composition occurs roughly in the range of 25 nm (Fig. 3c), while for the intensity minima the corresponding range is only for 10 nm (Fig. 3d). The differences in the observed range and oxygen/nitrogen content originates from the DLIL treatment, which likely is the result of the interference phenomenon. The range/thickness of the oxide/oxynitride layer is greater in the laser maxima (bottom) as a result of much higher temperature operating in these positions compared to in the minima (top). Molten material from the bottom of the grooves is relocated toward intensity minima regions where temperature is much lower. At minima intensity positions molten material is cooled faster which significantly reduce diffusion rates of nitrogen and oxygen. A similar effect has also been observed in other studies on DLIL-treated (otherwise known as Direct Laser Interference Patterning – DLIP) materials such as steel and pure aluminum [42,43]. Although, the reported results from the literature are obtained on other metallic materials, the conclusions and correlation between intensity and layer thickness are rather similar with our APT results.

According to the literature, the presence of nitrogen in the titanium oxide layer or a multilayer structure of the titanium oxide/nitride formed on the DLIL-treated titanium may influence surface properties, such as wettability [44–46] as well as corrosion passivation in biological solutions [47–49]. Presence of oxygen and nitrogen in titanium lead to a much stronger effect of solution strengthening compared to the basic alloying elements [50] which may also affect the mechanical properties of such surfaces, and thus the tribological properties.

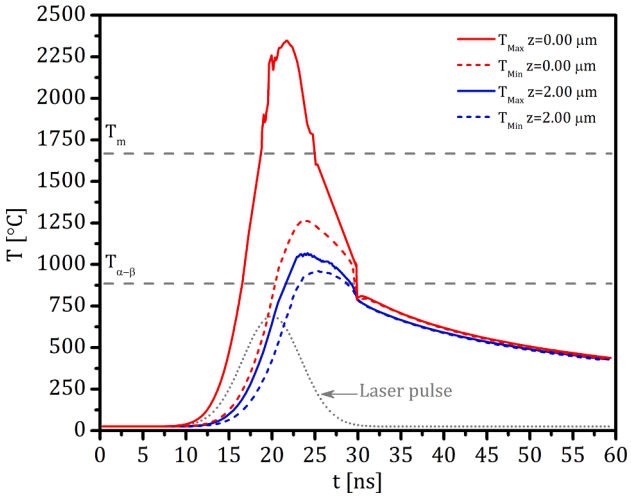

Fig. 4. Temperature evolution for maxima (T_{Max}, solid line) and minima (T_{Min}, dashed line) interference positions obtained from thermal simulation of Ti surface during laser treatment (0.35 J cm^{-2}, 8 ns pulse duration) at the surface ($z = 0.00$ µm, red lines) and at a depth of $z = 2.00$ µm (blue lines). The laser pulse intensity distribution in time is, schematically, presented (dotted grey line). The melting temperature (T_m) and phase transition temperature ($T_{\alpha-\beta}$) are also shown in the figure.

3.2. Thermal simulations

To determine the temperature distribution of the DLIL-modified titanium and to confront our APT experimental measurements, thermal simulations for the applied laser setup were performed. Fig. 4 presents the simulated temperature at the maxima (T_{Max}) and minima (T_{Min}) interference positions during one laser shot at the surface ($z = 0.00$ μm, red lines) and at a depth of 2 μm (blue lines).

The surface of the DLIL-modified titanium is locally melted at the maxima interference region and temperature reaches >2380°C. At the minima intensity temperature is >1200°C and remains below the melting point (T_m) but higher than the temperature needed for phase transition. The temperature of phase transition ($T_{\alpha-\beta}$, $\alpha \rightarrow \beta$) is still reached at depth of 2 μm at the maxima interference regions (>882°C). This result is in good agreement with our previous study [7] and existence of a 1.5 μm thick continuous layer consisting of lamellar grains in laser modified samples. The characteristic shape of the lath-like grains is typical for Ti cooled from the β stability region or higher temperatures.

Our thermal calculations showed that at the maxima intensity position temperature reaches the transient nitridation curve at >2350°C. However, as identified in the APT measurements, the N-enriched phase for both positions is a mixture of oxygen and nitrogen phases and not a pure TiN phase. Laser processing, due to the high heating/cooling rates, is a non-equilibrium process, thereby occurring phases may differ from these anticipated by phase diagrams. Nonetheless, periodically altered surface film thickness and inhomogeneity of chemical composition after DLIL treatment must be taken into consideration during intentional tailoring of the surface topography on commercially available implants.

4. Conclusions

This study demonstrates that APT is a suitable technique for analyzing the chemical composition and its changes both laterally, to see the effect of minimum and maximum interference intensity, as well as in depth of DLIL-modified titanium. The APT measurements clearly demonstrate that for both intensity positions, two separate layers are formed having an oxygen-rich layer on the top followed by a nitrogen-rich layer underneath. The thickness of the double layer depends on the local laser intensity at the surface, which varies periodically as a result of interference. Uneven temperature distribution, as shown by additional thermal simulations, on the titanium surface during DLIL treatment creates inhomogeneity in the chemical composition and periodically modulated film thickness. It is believed that an uneven temperature distribution on the titanium surface during DLIL treatment creates inhomogeneity in the chemical composition. In the context of the biomedical applications, DLIL surface treatment allows for intended formation of specific surface topography on pre-modified titanium as well as modification of surface chemistry without any additional steps.

CRediT authorship contribution statement

D. Kuczyńska-Zemła: Conceptualization, Methodology, Formal analysis, Investigation, Writing - original draft, Writing - review & editing, Visualization, Project administration, Funding acquisition. **G. Sundell:** Methodology, Formal analysis, Investigation, Writing - original draft, Writing - review & editing. **M. Zemła:** Methodology, Investigation, Formal analysis, Writing - review & editing. **M. Andersson:** Conceptualization, Formal analysis, Writing - original draft, Writing - review & editing, Supervision. **H. Garbacz:** Conceptualization, Formal analysis, Writing - original draft, Supervision, Funding acquisition.

Declaration of Competing Interest

The authors declare that they have no known competing financial interests or personal relationships that could have appeared to influence the work reported in this paper.

Acknowledgments

This work was supported by the National Science Centre Poland under ETIUDA project No. 2019/32/T/ST5/00377. The authors would like to thank Gustav Eriksson for assistance with the FIB-SEM sample preparation. The authors are also very grateful to Professor Jan Marczak, who sadly passed away, for his contribution to the laser treatment methodology and enormous technical support.

Appendix A. Supplementary material

Supplementary data associated with this article can be found, in the online version, at https://doi.org/10.1016/j.apsusc.2021.150193.

References

[1] S. Alamri, B. Krupop, T. Steege, A.I. Aguilar Morales, V. Lang, S. Storm, F. Schell, C. Zwahr, C. Kracht, M. Bieda, B. Voisiat, U. Klotzbach, A.F. Lasagni, T. Kunze, Quo Vadis surface functionalization: How direct laser interference patterning tackle productivity and flexibility in industrial applications, Proc. SPIE - Int. Soc. Opt. Eng. 10906 (2019) 27, https://doi.org/10.1117/12.2514209.

[2] M. D'Alessandria, A. Lasagni, F. Mücklich, Direct micro-patterning of aluminum substrates via laser interference metallurgy, Appl. Surf. Sci. 255 (2008) 3210–3216, https://doi.org/10.1016/j.apsusc.2008.09.018.

[3] A. Lasagni, M. D'Alessandria, R. Giovanelli, F. Mücklich, Advanced design of periodical architectures in bulk metals by means of Laser Interference Metallurgy, Appl. Surf. Sci. 254 (4) (2007) 930–936, https://doi.org/10.1016/j.apsusc.2007.08.010.

[4] A.F. Lasagni, C. Gachot, K.E. Trinh, M. Hans, A. Rosenkranz, T. Roch, S. Eckhardt, T. Kunze, M. Bieda, D. Günther, V. Lang, F. Mücklich, Direct laser interference patterning, 20 years of development: from the basics to industrial applications, Laser-based Micro- Nanoprocess. XI 10092 (2017) 1009211, https://doi.org/10.1117/12.2252595.

[5] A. Rosenkranz, M. Hans, C. Gachot, A. Thome, S. Bonk, F. Mücklich, Direct laser interference patterning: Tailoring of contact area for frictional and antibacterial properties, Lubricants 4 (1) (2016), https://doi.org/10.3390/lubricants4010002.

[6] C. Zwahr, B. Voisiat, A. Welle, D. Günther, A.F. Lasagni, One-Step Fabrication of Pillar and Crater-Like Structures on Titanium Using Direct Laser Interference Patterning, Adv. Eng. Mater. 1800160 (2018) 1–9, https://doi.org/10.1002/adem.201800160.

[7] D. Kuczyńska-Zemła, P. Kwaśniak, A. Sotniczuk, M. Spychalski, P. Wieciński, J. Zdunek, R. Ostrowski, H. Garbacz, Microstructure and mechanical properties of titanium subjected to direct laser interference lithography, Surf. Coatings Technol. 364 (2019) 422–429, https://doi.org/10.1016/j.surfcoat.2019.02.026.

[8] L. Zhao, Z. Wang, J. Zhang, L. Cao, L. Li, Y. Yue, D. Li, Antireflection silicon structures with hydrophobic property fabricated by three-beam laser interference, Appl. Surf. Sci. 346 (2015) 574–579, https://doi.org/10.1016/j.apsusc.2015.04.058.

[9] C. Zwahr, D. Günther, T. Brinkmann, N. Gulow, S. Oswald, M.G. Holthaus, A. F. Lasagni, Laser Surface Pattering of Titanium for Improving the Biological Performance of Dental Implants, Adv. Healthc. Mater. 1600858 (2017) 1–9, https://doi.org/10.1002/adhm.201600858.

[10] D. Kuczyńska-Zemła, E. Kijeńska-Gawrońska, M. Pisarek, P. Borowicz, W. Swieszkowski, H. Garbacz, Effect of laser functionalization of titanium on bioactivity and biological response, Appl. Surf. Sci. 525 (2020) 146492, https://doi.org/10.1016/j.apsusc.2020.146492.

[11] D. Wang, Z. Wang, Z. Zhang, Y. Yue, D. Li, C. Maple, Direct modification of silicon surface by nanosecond laser interference lithography, Appl. Surf. Sci. 282 (2013) 67–72, https://doi.org/10.1016/j.apsusc.2013.05.042.

[12] R. Vilar, Laser Surface Modification of Biomaterials Techniques and Applications, 2016. doi: 10.1016/B978-0-08-100883-6.00006-X.

[13] A.I. Aguilar-Morales, S. Alamri, T. Kunze, A.F. Lasagni, Influence of processing parameters on surface texture homogeneity using Direct Laser Interference Patterning, Opt. Laser Technol. 107 (2018) 216–227, https://doi.org/10.1016/j.optlastec.2018.05.044.

[14] M. Rahmati, E.A. Silva, J.E. Reseland, C.A. Heyward, H.J. Haugen, Biological responses to physicochemical properties of biomaterial surface, Chem. Soc. Rev. 49 (15) (2020) 5178–5224, https://doi.org/10.1039/d0cs00103a.

[15] S. Bauer, P. Schmuki, K. Von Der Mark, J. Park, Engineering biocompatible implant surfaces Part I: Materials and surfaces, Prog. Mater. Sci. 58 (3) (2013) 261–326, https://doi.org/10.1016/j.pmatsci.2012.09.001.

[16] J. Dias Corpa Tardelli, M. Lima da Costa Valente, T. Theodoro de Oliveira, A. Cândido dos Reis, Influence of chemical composition on cell viability on titanium surfaces: A systematic review, J. Prosthet. Dent. (2020) 1–5, https://doi.org/10.1016/j.prosdent.2020.02.001.

[17] C. Sittig, M. Textor, N.D. Spencer, M. Wieland, P.H. Vallotton, Surface characterization of implant materials CP Ti, Ti-6Al-7Nb and Ti-6Al-4V with different pretreatments, J. Mater. Sci. Mater. Med. 10 (1) (1999) 35–46, https://doi.org/10.1023/A:1008840026907.

[18] E. Mccafferty, J.P. Wightman, An X-ray photoelectron spectroscopy sputter profile study of the native air-formed oxide film on titanium, Appl. Surf. Sci. 143 (1999) 92–100.
[19] O. Seddiki, C. Harnagea, L. Levesque, D. Mantovani, F. Rosei, Evidence of antibacterial activity on titanium surfaces through nanotextures, Appl. Surf. Sci. 308 (2014) 275–284, https://doi.org/10.1016/j.apsusc.2014.04.155.
[20] F. Torrent, L. Lavisse, P. Berger, J.M. Jouvard, H. Andrzejewski, G. Pillon, S. Bourgeois, M.C. Marco De Lucas, Wavelength influence on nitrogen insertion into titanium by nanosecond pulsed laser irradiation in air, Appl. Surf. Sci. 278 (2013) 245–249, https://doi.org/10.1016/j.apsusc.2012.11.110.
[21] L. Lavisse, J.M. Jouvard, J.P. Gallien, P. Berger, D. Grevey, P. Naudy, The influence of laser power and repetition rate on oxygen and nitrogen insertion into titanium using pulsed Nd:YAG laser irradiation, Appl. Surf. Sci. 254 (4) (2007) 916–920, https://doi.org/10.1016/j.apsusc.2007.07.204.
[22] C. Zwahr, A. Welle, T. Weingärtner, C. Heinemann, B. Kruppke, N. Gulow, M. Holthaus, A.F. Lasagni, Ultrashort Pulsed Laser Surface Patterning of Titanium to Improve Osseointegration of Dental Implants, Adv. Eng. Mater. 1900639 (2019) 1–11, https://doi.org/10.1002/adem.201900639.
[23] D. Kuczyńska, P. Kwaśniak, M. Pisarek, P. Borowicz, H. Garbacz, Influence of surface pattern on the biological properties of Ti grade 2, Mater. Charact. 135 (2018) 337–347, https://doi.org/10.1016/j.matchar.2017.09.024.
[24] H. Garbacz, P. Wieciński, D. Kuczyńska, D. Kubacka, K. Kurzydłowski, The effect of grain size on the surface properties of titanium grade 2 after different treatments, Surf. Coatings Technol. 335 (2018) 13–24, https://doi.org/10.1016/j.surfcoat.2017.12.005.
[25] K. Stiller, L. Viskari, G. Sundell, F. Liu, M. Thuvander, H.O. Andrén, D.J. Larson, T. Prosa, D. Reinhard, Atom probe tomography of oxide scales, Oxid. Met. 79 (3–4) (2013) 227–238, https://doi.org/10.1007/s11085-012-9330-6.
[26] G. Sundell, C. Dahlin, M. Andersson, M. Thuvander, The bone-implant interface of dental implants in humans on the atomic scale, Acta Biomater. 48 (2017) 445–450, https://doi.org/10.1016/j.actbio.2016.11.044.
[27] J. Karlsson, G. Sundell, M. Thuvander, M. Andersson, Atomically resolved tissue integration, Nano Lett. 14 (8) (2014) 4220–4223, https://doi.org/10.1021/nl501564f.
[28] R. Junker, A. Dimakis, M. Thoneick, J.A. Jansen, Effects of implant surface coatings and composition on bone integration: A systematic review, Clin. Oral Implants Res. 20 (SUPPL. 4) (2009) 185–206, https://doi.org/10.1111/j.1600-0501.2009.01777.x.
[29] D. Kuczyńska, P. Kwaśniak, J. Marczak, J. Bonarski, J. Smolik, Laser surface treatment and the resultant hierarchical topography of Ti grade 2 for biomedical application, Appl. Surf. Sci. 390 (2016) 560–569, https://doi.org/10.1016/j.apsusc.2016.08.105.
[30] S. Ber, G. Torun Köse, V. Hasirci, Bone tissue engineering on patterned collagen films: An in vitro study, Biomaterials 26 (14) (2005) 1977–1986, https://doi.org/10.1016/j.biomaterials.2004.07.007.
[31] X.F. Walboomers, H.J. Croes, L.A. Ginsel, J.A. Jansen, Growth behavior of fibroblasts on microgrooved polystyrene, Biomaterials 19 (20) (1998) 1861–1868, https://doi.org/10.1016/S0142-9612(98)00093-3.
[32] K. Anselme, M. Bigerelle, B. Noël, A. Iost, P. Hardouin, Effect of grooved titanium substratum on human osteoblatic cell adhesion, J. Biomed. Mater. Res. 60 (4) (2002) 529–540, https://doi.org/10.1002/jbm.10101.
[33] M.K. Miller, K.F. Russell, G.B. Thompson, Strategies for fabricating atom probe specimens with a dual beam FIB, Ultramicroscopy 102 (4) (2005) 287–298, https://doi.org/10.1016/j.ultramic.2004.10.011.
[34] K. Thompson, D. Lawrence, D.J. Larson, J.D. Olson, T.F. Kelly, B. Gorman, In situ site-specific specimen preparation for atom probe tomography, Ultramicroscopy 107 (2–3) (2007) 131–139, https://doi.org/10.1016/j.ultramic.2006.06.008.
[35] X. Wang, B. Langelier, F.A. Shah, A. Korinek, M. Bugnet, A.P. Hitchcock, A. Palmquist, K. Grandfield, Biomineralization at Titanium Revealed by Correlative 4D Tomographic and Spectroscopic Methods, Adv. Mater. Interfaces 5 (14) (2018) 1–9, https://doi.org/10.1002/admi.201800262.
[36] L. Nánai, R. Vajtai, T.F. George, Laser-induced oxidation of metals: State of the art, Thin Solid Films 298 (1–2) (1997) 160–164, https://doi.org/10.1016/S0040-6090(96)09390-X.
[37] A.M. Chaze, C. Coddet, The role of nitrogen in the oxidation behaviour of titanium and some binary alloys, J. Less-Common Met. 124 (1–2) (1986) 73–84, https://doi.org/10.1016/0022-5088(86)90478-9.
[38] C. Zeng, H. Wen, B. Zhang, P.T. Sprunger, S.M. Guo, Diffusion of oxygen and nitrogen into titanium under laser irradiation in air, Appl. Surf. Sci. 505 (August 2019) (2020) 144578, https://doi.org/10.1016/j.apsusc.2019.144578.
[39] L. Lavisse, P. Berger, M. Cirisan, J.M. Jouvard, S. Bourgeois, M.C. Marco De Lucas, Influence of laser-target interaction regime on composition and properties of surface layers grown by laser treatment of Ti plates, J. Phys. D: Appl. Phys. 42 (2009) 245303, https://doi.org/10.1088/0022-3727/42/24/245303.
[40] E. Carpene, P. Schaaf, M. Han, K.P. Lieb, M. Shinn, Reactive surface processing by irradiation with excimer laser, Nd:YAG laser, free electron laser and Ti:sapphire laser in nitrogen atmosphere, Appl. Surf. Sci. 186 (1–4) (2002) 195–199, https://doi.org/10.1016/S0169-4332(01)00625-0.
[41] A.L. Thomann, A. Basillais, M. Wegscheider, C. Boulmer-Leborgne, A. Pereira, P. Delaporte, M. Sentis, T. Sauvage, Chemical and structural modifications of laser treated iron surfaces: Investigation of laser processing parameters, Appl. Surf. Sci. 230 (1–4) (2004) 350–363, https://doi.org/10.1016/j.apsusc.2004.02.060.
[42] A. Rosenkranz, L. Reinert, C. Gachot, H. Aboufadl, S. Grandthyll, K. Jacobs, F. Müller, F. Mücklich, Oxide Formation, Morphology, and Nanohardness of Laser-Patterned Steel Surfaces, Adv. Eng. Mater. 17 (8) (2015) 1234–1242, https://doi.org/10.1002/adem.201400487.
[43] M. D'Alessandria, F. Mücklich, Tailoring the chemical behavior of aluminum for selective etching by laser interference metallurgy, Appl. Phys. A Mater. Sci. Process. 98 (2) (2010) 311–320, https://doi.org/10.1007/s00339-009-5398-5.
[44] D. Mardare, D. Luca, C.M. Teodorescu, D. Macovei, On the hydrophilicity of nitrogen-doped TiO 2 thin films, Surf. Sci. 601 (2007) 4515–4520, https://doi.org/10.1016/j.susc.2007.04.156.
[45] E.A. De Souza Filho, E.F. Pieretti, R.T. Bento, M.F. Pillis, Effect of nitrogen-doping on the surface chemistry and corrosion stability of TiO2 films, J. Mater. Res. Technol. 9 (1) (2020) 922–934, https://doi.org/10.1016/j.jmrt.2019.11.032.
[46] Z. Sun, V.F. Pichugin, K.E. Evdokimov, M.E. Konishchev, M.S. Syrtanov, V. N. Kudiiarov, K. Li, S.I. Tverdokhlebov, Effect of nitrogen-doping and post annealing on wettability and band gap energy of TiO2 thin film, Appl. Surf. Sci. 500 (144048) (2020), https://doi.org/10.1016/j.apsusc.2019.144048.
[47] D. Kuczyńska-Zemła, A. Sotniczuk, M. Pisarek, A. Chlanda, H. Garbacz, Corrosion Behavior of Titanium Modified by Direct Laser Interference Lithography, Surf. Coat. Technol. 418 (2021) 127219, https://doi.org/10.1016/j.surfcoat.2021.127219.
[48] H. Wang, R. Zhang, Z. Yuan, X. Shu, E. Liu, Z. Han, A comparative study of the corrosion performance of titanium (Ti), titanium nitride (TiN), titanium dioxide (TiO2) and nitrogen-doped titanium oxides (N–TiO2), as coatings for biomedical applications, Ceram. Int. 41 (9) (2015) 11844–11851, https://doi.org/10.1016/j.ceramint.2015.05.153.
[49] J. Liu, Y. Lou, C. Zhang, S. Yin, H. Li, D. Sun, X. Sun, Improved corrosion resistance and antibacterial properties of composite arch-wires by N-doped TiO2 coating, RSC Adv. 7 (69) (2017) 43938–43949, https://doi.org/10.1039/c7ra06960j.
[50] P. Kwasniak, H. Garbacz, K.J. Kurzydlowski, Solid solution strengthening of hexagonal titanium alloys: Restoring forces and stacking faults calculated from first principles, Acta Mater. 102 (2016) 304–314, https://doi.org/10.1016/j.actamat.2015.09.041.